is attributed to tidal disruption, though a plausible mechanism for this has not been proposed. In May 2002, we undertook a 4-night AF2/WYFFOS run to obtain large-radius stellar velocities in UMi, with the aim of fitting for the halo shape and orbital anisotropy using our α, ν models. However, 2.5 nights were clouded out, and poor seeing limited the quality of the data of the remaining 1.5 nights.

Though our data was insufficient for detailed modelling, we were nevertheless able to obtain a number of velocities in the vicinity of UMi's second density peak. After combining our data set with previously published UMi velocities, we noted that the velocity histogram of the clump appeared narrower than the dispersion of UMi as a whole (Kleyna et al., 2003). Accordingly, we modelled UMi's velocity distribution as the sum of two Gaussians: a Gaussian subpopulation with adjustable normalisation, width and mean, and an 8.8 km s^{-1} Gaussian representing the bulk of UMi's stars. We then scanned the face of UMi to determine where there was a signature of a kinematical subpopulation. As suggested by the histograms, only the region near the second clump contained statistically significant (p=99.45%) evidence of a second kinematical population (Figure 2).

We note that a dynamically coherent population can survive inside a cored halo, because sinusoidal orbits in the (nearly) harmonic potential of a core do not diverge over time. However, kinematical substructure would be quickly smeared out if UMi's halo had a density cusp, as predicted by CDM. Detailed dynamical simulations demonstrate that a cold clump could survive for a Hubble time in a 5×10^7 $M_\odot$ UMi-like dSph if the halo has a core larger than ~500 pc. If the halo has a cusp, however, all evidence of substructure is erased within several hundred million years.

Summary

Using large-radius velocity data obtained using AF2/WYFFOS, we show that the Draco dSph possesses an anisotropic velocity distribution and a dark halo that is isothermal in the limit of large radii. In Ursa Minor, we show that the second peak in the stellar density has a cold kinematical signature. This signature strongly suggests that the feature is a persistent clump sloshing back and forth within a dark matter core, and is inconsistent with the cusped halos that are predicted by Cold Dark Matter theory.¤

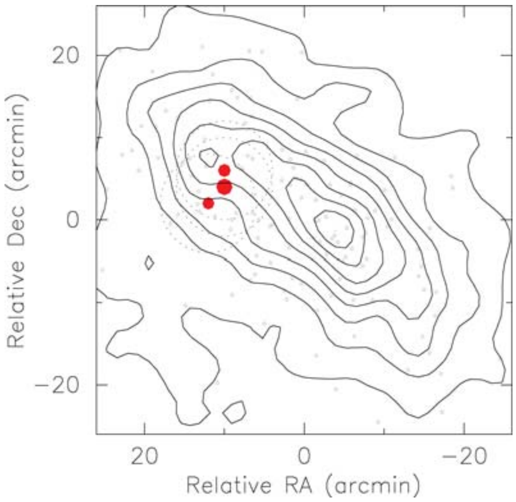

Figure 2. Result of search for kinematic sub-populations in UMi. Coutours are linearly spaced stellar isopleths; the second peak of UMi's stellar population is visible above and to the left of the centre. Gray stars are UMi red giant branch member stars with measured velocities. The filled circles represent points where a model with a kinematically cold sub-population is at least 1000 times more likely than a model composed of a single 8.8 km s^{-1} Gaussian. The size of each dot is proportional to the logarithm of the relative likelihood.

Jan Kleyna (kleyna@ast.cam.ac.uk)

References:

Aaronson, M., 1983, *ApJ*, **266**, L11.

Armandroff, T. E., Olszewski, E. W., Pryor, C., 1995, *AJ*, **110**, 2131.

Hargreaves, J. C., Gilmore, G., Irwin, M. J., Carter, D., 1996, *MNRAS*, **282**, 305.

Kleyna, J. T., Wilkinson, M. I., Evans, N. W., Gilmore G., 2001, *ApJ*, **563**, L115.

Kleyna, J. T., Wilkinson, M. I., Gilmore G., Evans, N. W., 2003, *ApJ*, **588**, L21.

Wilkinson M. I., Kleyna, J. T., Evans, N. W., Gilmore G., 2002, *MNRAS*, **330**, 778.

The SAURON Deep Field: Investigating the Diffuse Lyman-α Halo of "Blob1" in SSA 22

R. G. Bower[1], S. L. Morris[1], R. Bacon[2], R. Wilman[1], M. Sullivan[1], S. Chapman[3], R. L. Davies[4], P. T. de Zeeuw[5]

1: Physics Department, University of Durham. 2: CRAL-Observatoire, Lyon. 3: California Institute of Technology. 4: Dept. of Astrophysics, University of Oxford. 5: Sterrewacht Leiden.

Recent studies of star-forming objects in the early universe, measuring their clustering properties and determining their luminosity functions, have shown that these galaxies are key to understanding the star formation and metal enrichment history of the universe and the role of galactic "super-winds" in regulating the conversion of baryons into stars.

In this article, we describe how, using the SAURON integral field spectrograph, we study the formation of the most massive galaxies in the Universe. The primary target is the bright Ly-α emission line halo in the conspicuous SSA 22 super-cluster at z=3.07–3.11 (Steidel et al., 2000). The highly-obscured very luminous submillimeter galaxy found by SCUBA near the centre of this halo probably is an example of a forming massive elliptical galaxy (Chapman et al., 2001).

Using SAURON, we can map the three-dimensional velocity structure of the SSA 22 'blob 1' halo. This allows us to probe the nature of the ionised gas surrounding the SCUBA source, gaining insight into the origin of the diffuse halo (is it primordial material infalling onto the central object, or material expelled during a violent star burst), the mass of its dark matter halo, and the energetics of any super-wind being expelled from the galaxy. We can also trace the large scale structure surrounding the central source, and investigate whether similar haloes are surrounding other galaxies in the field. The answers to these questions will allow us to understand how galaxy formation is regulated in massive galaxies in the high-redshift Universe. They offer key insight into the "feedback" process and will help explain why less than 10% of the baryon content of the universe ever forms into stars (the "cosmic cooling crisis"; Cen & Ostriker, 1999; Balogh et al., 2001).

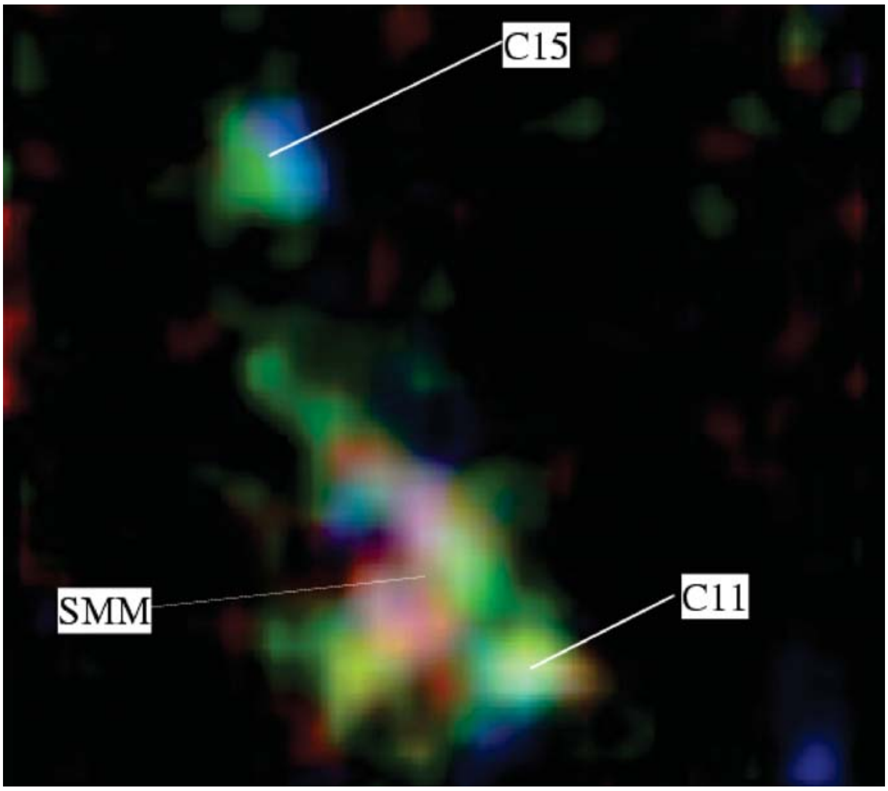

Figure 1. A colour representation of the wavelength shifts of Ly-α emission in the diffuse halo of SSA 22 'blob 1'. A simple interpretation of the image is that red, green and blue channels represent the red-shifted and blue-shifted motions of the ionised material in the halo. The positions of the two Lyman break galaxies C11 and C15 are marked, along with the position of the submillimeter source (SMM). The area shown is 37″×46″.

This is new ground for the SAURON instrument. Although it was designed to study the dynamics and stellar populations of nearby elliptical galaxies, we will show that it can very effectively be used to study low surface brightness emission features only detectable in long integrations. These observations offer a fore-taste of the deep field observations that can be made with the VIMOS and MUSE integral field spectrographs on 8 m telescopes.

The Data-Cube

The SAURON instrument is a high throughput integral field spectrograph (Bacon et al., 2001) that is currently operated on the William Herschel Telescope. It was designed and built by a partnership between Lyon, Durham and Leiden with the main objective of studying the dynamics and stellar populations of early-type galaxies (de Zeeuw et al., 2002). It combines a wide field (41″×33″ sampled at 0.95″) with a relatively high spectral resolution (4 Å FWHM, equivalent to σ=100 km s^{-1} in the target rest frame). The instrument achieves this by compromising on the total wavelength coverage, which is limited to 4810 to 5400 Å. This spatial and spectral sampling ensure that low surface brightness features are not swamped by read-out noise. However, the limited spectral coverage means that it is only possible to study the Ly-α emission from systems at redshifts between z=2.95 and 3.45. Fortunately, the SSA 22 supercluster lies within this redshift range. The sky background is devoid of strong night sky emission in the Sauron wavelength range. For these observations, the SAURON grating was upgraded with a VPH unit giving an overall system throughput of 20%.

Sauron was used to observe the SSA 22 source for a total of 9 hours, spread over 3 nights in July 2002. The raw data was reduced using the `XSauron` software. The extraction procedure uses a model for the instrumental distortions to locate each of the spectra, and to then extract them using optimal weighting. The extraction process takes into account the flux overlap between adjacent spectra. To remove small flat-field and sky subtraction residuals, a super-flat was created using the eighteen 30 min individual exposures. This procedure improved the flat field accuracy up to 1% RMS. Each individual datacube was then registered to a common spatial location using the faint star in the south east of the field and then merged into the final data-cube. To produce the map of Ly-α emission, we subtract the continuum, using a low order polynomial fit to the full wavelength range. The end result is a 3-D (x, y, λ) map of the Ly-α emission from the region.

Results

Three dimensional data of this type must be carefully visualised in order to extract the maximum information from the data. We started by creating a colour projection of the data cube shown in Figure 1. In this view, the red, green and blue colour channels have been created from the data in the wavelength ranges 4976.05, 4964.75, 4988.70. Each channel is 5.75 Å wide (350 km s^{-1} in the system rest frame). The image has also been smoothed spatially with a Gaussian of 1″ width. We have marked the positions of the Lyman break galaxies, C11 and C15, identified by Steidel et al. (1996) and the location of the sub-mm source identified by Chapman et al. (2003) (see below). The data-cube can alternatively be viewed as a sequence of wavelength slices as shown in Figure 2, or these slices can be combined together to make an animation.

Many striking structures can be clearly seen in the main halo. The overall width of the emission is very broad (~1500 km s^{-1} FWHM) but separate emission structures can be identified. If we interpret the wavelength shift as a Doppler shift, the systems differ in velocity by a few hundred km s^{-1}. There is significant velocity asymmetry in the emission region around the Lyman break galaxy C11 and across the main halo. The morphology of the diffuse emission also becomes clear in these velocity slices: particularly interesting is the depression seen near the centre of the halo (this is partially filled by redshifted emission), and the diffuse extension of the halo towards the nearby Lyman break galaxy C15. C15 itself is centred in a separate but much smaller halo. There is a clear E–W velocity shift across this 'mini-halo'. We discuss each of these features below.

The optical counter-part of the sub-mm source has been identified by Chapman et al. (2003) after detecting the associated CO emission. To locate the emission relative to the SCUBA source more precisely, we aligned the IFU data cube and the HST STIS image of Chapman et al. using the locations of the alignment star and the Lyman break galaxies C11 and C15. Figure 3 shows the STIS image overlayed with the contours of the total Ly-α emission. This clearly shows the location of the sub-mm source close to the centre of the 'cavity' in the emission structure.

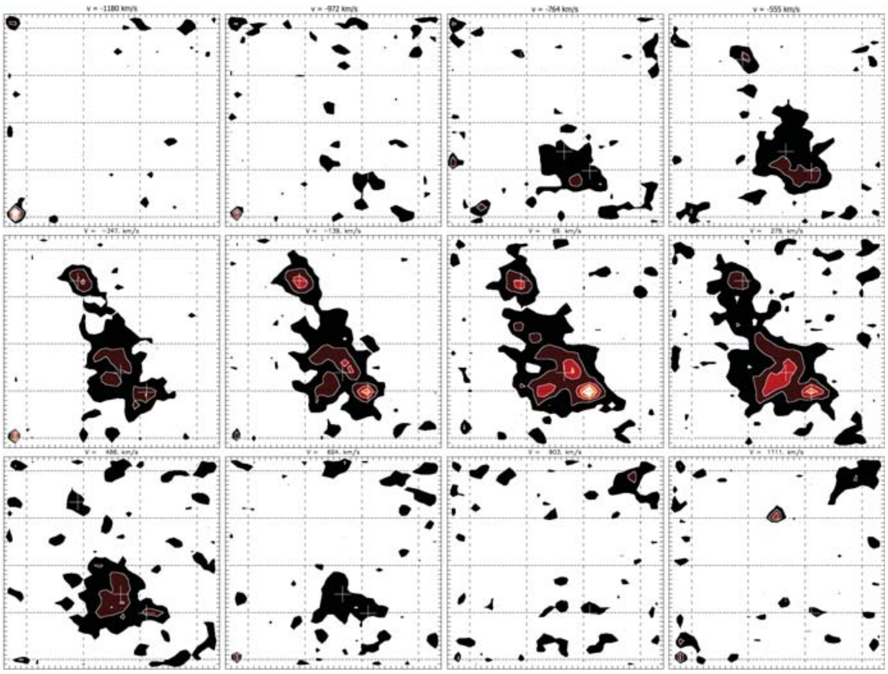

Figure 2. A sequence of contour plots showing the changing morphology of the Ly-α emission at different wavelengths. The velocity step between each map is 208 km s^{-1}, with each slice combining a 5.75 Å wavelength range so that alternate panels show independent data. Crosses mark the positions of Lyman break galaxies and the submillimeter source. The grid squares have a spacing of 8″.

Discussion

Below we divide our results into the separate features seen in our data and discuss some ideas for how we might interpret them. The interpretation is complicated because Ly-α is a resonant line. Thus shifts in the feature can appear both because of genuine gas motion and because photons diffuse in wavelength to escape from optically thick regions. In what follows we assume that bulk motion is the dominant source of line broadening.

– The main halo has a complex structure. Within the broad emission, there are many halo components. The variations in line width and velocity are inconsistent with a simple outflowing shell. The distribution is better modelled by distinct gas components, moving relative to each other with speeds of several hundred km s^{-1}. One (certainly naive) interpretation of the wavelength variations is that they reflect the free motions of separate gas clumps bound in a common gravitational potential.

– If the above were true, we could use the magnitude of the velocity differences to infer the halo mass within ~75 kpc (or 10″, the typical radius at which the clumps can be identified). If we assume that the clumps are on random orbits with a line of sight velocity dispersion of 500 km s^{-1}, this suggests a mass of order 1.3×10^{13} $M_{\odot}$, as expected for a small cluster. It is likely, however, that in fact the clumps have a net outflow or inflow, or are subject to drag from the intergalactic medium (IGM). This makes the mass estimate uncertain.

– Figure 3 shows the relative location of the emission-line halo and the optical counterpart of the strong sub-mm source (Chapman et al., 2001; 2003). The overlay suggests that the sub-mm source may be located at the centre of a 'cavity' in the Ly-α emission. There are several possible interpretations of this cavity. (1) It may be a genuine cavity in the ionised gas distribution. This might be evidence for a strong wind being blown away from the central

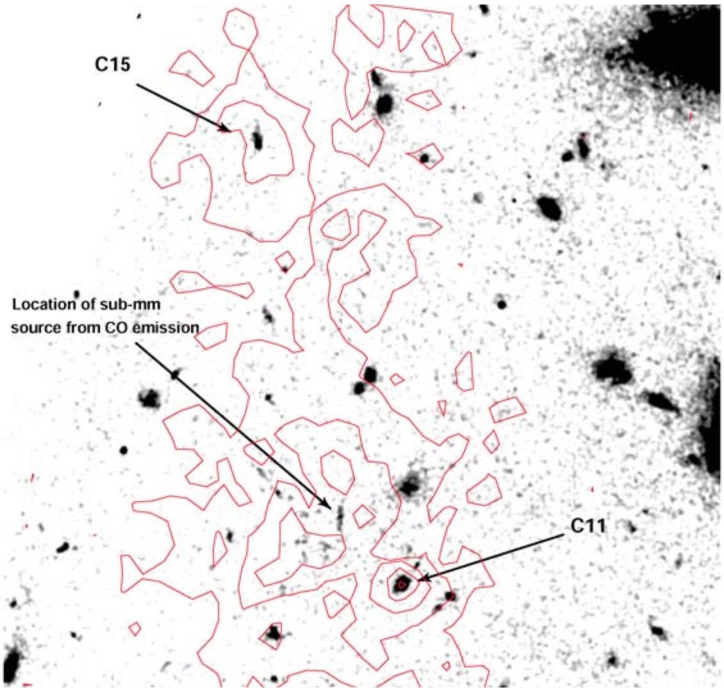

Figure 3. A deep STIS image of the SSA 22 'blob 1' region showing the position for the SCUBA counterpart (Chapman et al., 2003) relative to the total Ly-α emission (contours). The sub-mm source may lie in a 3-D cavity in the emission (compare contours with Figure 1). The Lyman break galaxies C15 and C11 are marked. Their distinct haloes are clearly seen in the 3-D data set.

sub-mm source. This would obviously not be consistent with the more distant material being discrete gas clumps moving on orbits with their motion dominated by the gravitational potential. (2) The cavity may occur because the ionised gas in this region contains significant dust. As the Ly-α diffuses out of the region, it is strongly extincted. This would be consistent with redshifted emission being seen in this location (this wavelength is not resonantly scattered). This explanation is appealing since we know that the central SCUBA source has high extinction. (3) It is possible that we are seeing the optical equivalent of Wide Angle Tail radio sources, where line emission is coming from poorly collimated outflows from a central galaxy, which are then decelerated by the IGM, while the central source moves on through the IGM.

– The two other Lyman break galaxies embedded in the structure appear to have dynamically distinct haloes. This is particularly clear for C15, to the north of the main halo. Indeed there is faint emission that bridges between C15 and the central halo. A similar feature can also be discerned around C11. This is a surprising discovery that leads us to consider whether other Lyman break galaxies would also have extended Ly-α haloes.

– The mini-halo around the C15 Lyman break galaxy has its own characteristic velocity shear pattern. We can identify the morphology of this galaxy from the STIS imaging of Chapman et al. (2003). C15 is elongated at roughly 60 degrees (Figure 3) to the velocity shear seen in Ly-α. This, together with the morphology of the emission, makes it unlikely that the shear reflects the rotation of a conventional gas disk. Instead, the shear pattern is reminiscent of the super-wind outflows predicted from proto-galactic disks (Springel & Hernquist, 2002), and observed (on a smaller scale) in local starburst galaxies such as M82.

Next Steps

These observations clearly demonstrate the ability of deep integral field spectroscopy to detect low surface brightness emission from distant galaxies in the early universe. They give us fascinating insight into the nature and structure of the ionised halo of SSA 22-1. It is interesting to now see how far this powerful new technique can be taken. On the one hand it is fundamental to establish whether the diversity of structure seen in SSA 22-1 is a generic property of other highly luminous sub-mm galaxies, or whether the deep potential well of the SSA 22 super-cluster is necessary to produce emission of this luminosity and extent. It will also be important to determine whether other Lyman break galaxies show mini-haloes similar to C15.

Our observations with the SAURON spectrograph also lay out a path for forthcoming integral fields units. For example, OASIS, an adaptive optics optimised integral field spectrograph, could be used to complement SAURON by studing the higher surface brightness emission line regions in greater detail. The MUSE spectrograph being designed for the VLT will offer the ideal combination of all these instruments providing a combination of wide-field coverage, good spatial resolution and optimal spectral resolution.

Acknowledgments

We thank the SAURON instrument team for their support of this program, and for creating an instrument with the superb sensitivity of SAURON. RGB acknowledges the support of the Leverhulme foundation.¤

References:

Bacon et al., 2001, *MNRAS*, **326**, 23.

Balogh, Pearce, Bower & Kay, 2001, *MNRAS*, **326**, 1228.

Cen & Ostriker, 1999, *ApJ*, **519**, L109.

Chapman, et al., 2001, *ApJ*, **548**, 17.

Chapman et al., 2003, in prep.

de Zeeuw et al., 2002, *MNRAS*, **329**, 513.

Springel & Hernquist, 2003, *MNRAS*, **339**, 289.

Steidel, Giavalisco, Dickinson, Adelberger, 1996, *ApJ*, **462**, L17.

Richard Bower (r.g.bower@durham.ac.uk)